

Fun with the Sun: Modeling the Solar Atmosphere and Na D1 Line

LORRAINE NICHOLSON¹

¹*University of Florida
Department of Astronomy*

ABSTRACT

This project investigates stellar atmospheric properties through the lens of the Solar atmosphere. In part I, I use theoretical data from Fontenla et al. (1993) to explore how physical properties such as temperature, density, pressure, etc. vary with height in the Solar atmosphere. The atmosphere is composed of three main regimes which have distinct characteristics: photosphere, chromosphere, and corona. The photosphere is closest to the "surface" of the star at $\tau = 2/3$. As height increases from the stellar surface to the top of atmosphere, the optical depth (τ) decreases. The gas located at $\tau < 1$ leaves a distinct imprint on the stars Planck function. In other words, a stellar spectra is largely determined by the $\tau < 1$ region of the star. So, a deep understanding of stellar atmospheres is critical to the interpretation of stellar spectra. In part II, I use data from Allen (1976) to investigate the Solar spectrum itself and begin to set-up a model Solar atmosphere. Finally, in part III I model the Na D1 absorption line for the Solar spectrum.

1. PART I

1.1. Part A

The temperature profile resulting from the realistic Solar model is shown in Figure 1. The photosphere of the star is the coolest with temperature $\approx 6 \times 10^3$ K, the chromosphere is slightly warmer, and the star has the highest temperature in the corona where $T \approx 10^5$ K. The photosphere is near the "surface" of the star, because of it's relatively cool temperature it is responsible for producing the **absorption lines** we observe in Solar spectra. The warmer chromosphere produces **emission lines** due to Hydrogen being present in this layer.

1.2. Part B

Similarly, τ at 5000 Å as a function of temperature is shown in Figure 2. Also shown in Figure 2 is the result of the "grey atmosphere" solution derived from the Eddington-Milne approximation:

$$T(\tau) = T_{eff} \left(\frac{3}{4}\tau + \frac{1}{2} \right)^{1/4} \quad (1)$$

Where T_{eff} is the temperature at $\tau = 2/3$. The 'grey atmosphere' solution is a good match to the realistic model for τ close to 1. However, the 'grey atmosphere' solution is not a good approximation for $\tau \ll 1$. This reveals that the 'grey atmosphere' solution is only valid near the stellar surface.

1.3. Part C

The number density of Hydrogen, electrons, and protons are shown in Figure 3. In the photosphere, near the surface of the star, Hydrogen is dominant with $\approx 10^{17}$ n_H/cm³. Also in the photosphere, the number density of electrons is greater than protons. The number density of Hydrogen starts to decrease dramatically in the chromosphere, while the number density of electrons and protons are equal to each other in this region. The difference between n_H and n_e is smaller in this region, only about 3 orders of magnitude. All three number densities then drop-off in the Corona. The number densities decrease as the temperature increases, hinting at molecules becoming ionized in the outer layers of the atmospheres.

1.4. Part D

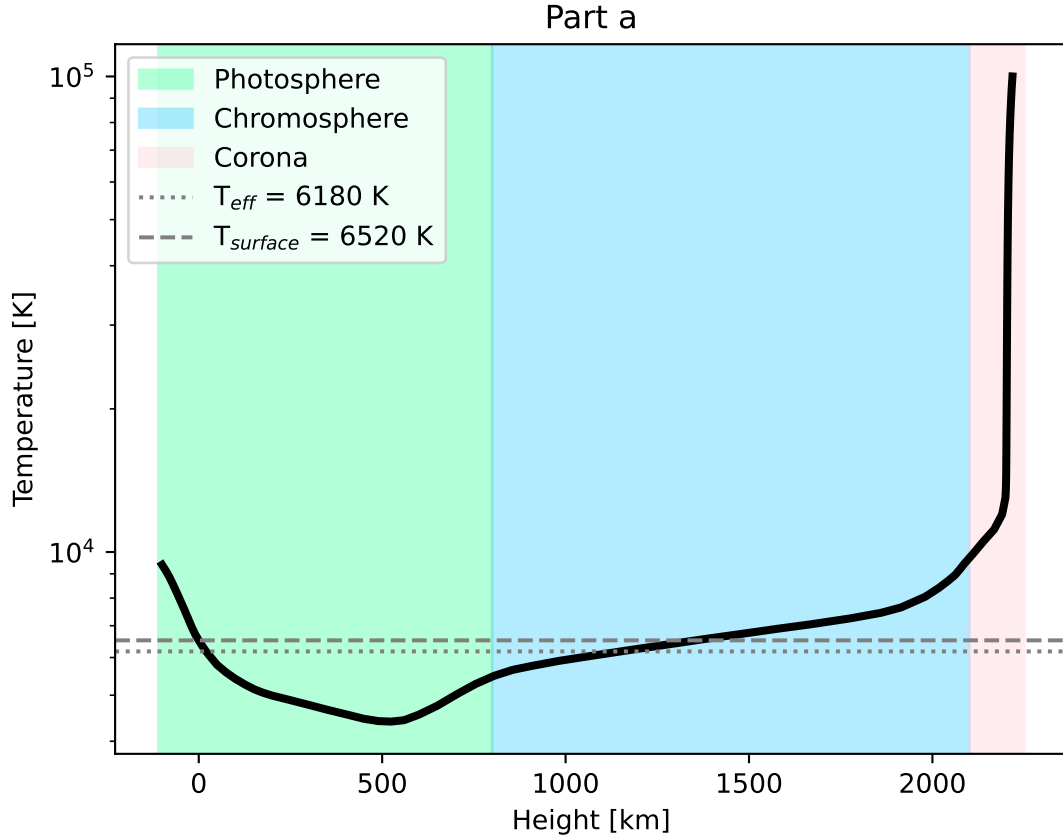


Figure 1. Temperature vs. Height. Temperature profile of the Sun's atmosphere. This figure reveals three main regimes of the Sun's atmosphere: The photosphere at heights $\approx 0 - 800$ km (green shaded region), the chromosphere at $\approx 800 - 2100$ km (blue shaded region), and the corona above ≈ 2100 km (pink shaded region). The dashed grey line is the surface temperature of the Sun, corresponding to $\tau = 1$. Based on this, you can tell that the stellar surface is at height = 0.0 km. The dotted grey line is the effective temperature of the Sun, corresponding to $\tau = 2/3$.

The density stratification is shown in Figure 4. The density is highest in the photosphere near the surface of the star, $\rho \approx 10^{-7}$ g/cm³. The density decreases exponentially in the chromosphere and reaches a minimum in the corona.

To estimate the density scale height, H_ρ , I fit the definition $\rho = \rho_0 e^{-h/H_\rho}$ to the curve, where $\rho_0 = \rho(h = 0)$. I found that $H_\rho \approx 130$ km is a good match to the model. Comparing this scale height to the radius of the Sun, $\frac{R_\odot}{H_\rho} = 5356.26$ therefore this is an extended spherical object and the plane parallel assumption is valid. Moreover, the height of the Solar atmosphere is 2218.2 km which is about 17 "scale heights" high.

1.5. Part E

The total pressure (P_{tot}) in the Solar atmosphere is shown in Figure 5. Also shown in Figure 5 is the gas pressure (P_{gas}) which I calculated from the ideal gas law:

$$PV = Nk_B T \quad (2)$$

I related this to the number density with $n = \frac{N}{V}$, therefore,

$$P_{gas} = (n_H + n_e)k_B T \quad (3)$$

Overall, P_{gas} is a good match to P_{tot} , with small deviations near the surface and larger deviations at the very top of the chromosphere and the corona. The deviations probably occur because there are other things that can contribute weakly to pressure such as radiation pressure and turbulence pressure, which I did not take into account for my calculation of P_{gas} .

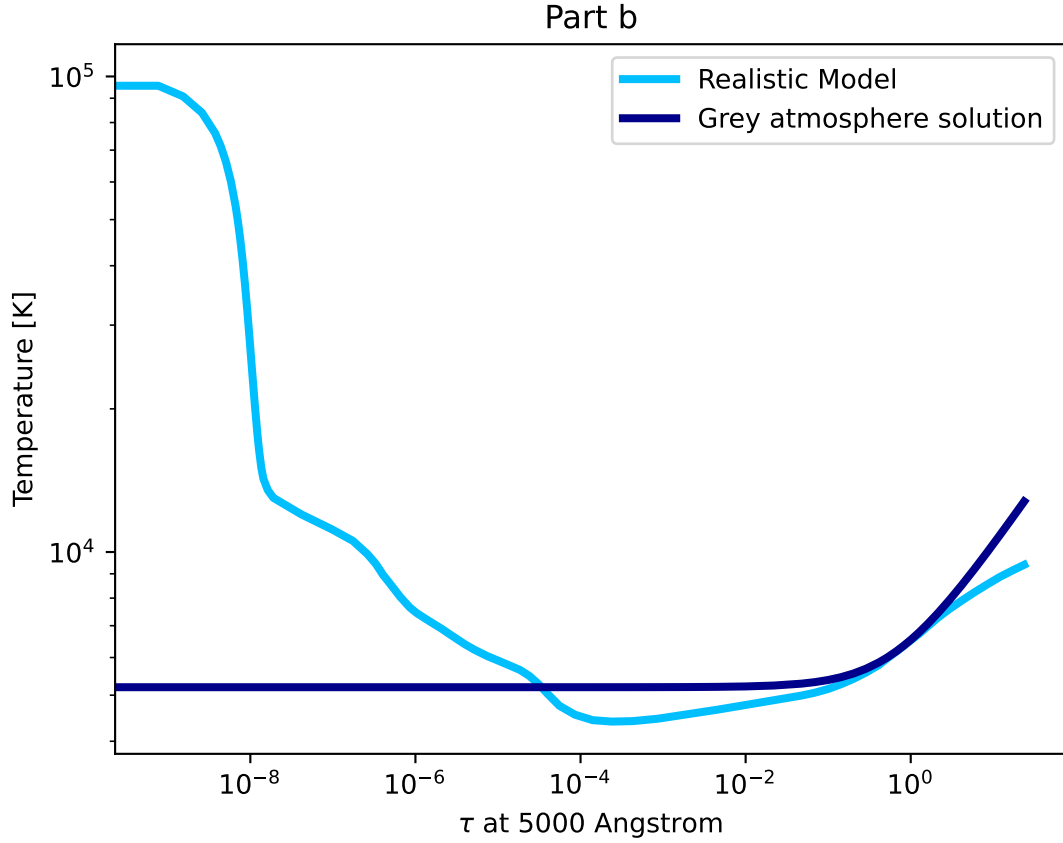


Figure 2. Temperature vs. τ at 5000 \AA . Temperature curve of the realistic model (light blue) and the "grey atmosphere" solution (dark blue). $\tau = 2/3$ corresponds to the "surface" of the star, and τ decreases as you move outward to the top of the atmosphere.

1.6. Part F

The ratio of P_{gas} to P_{tot} is defined by the variable β and is shown in Figure 6. This further shows that P_{gas} deviates from P_{tot} slightly in the photosphere, and the difference is most dramatic in the chromosphere. The differences likely arise because there are other contributors to pressure such as radiation pressure and turbulent pressure. The difference between the model β and my analytically calculated β likely arise because of the ideal gas law assumption not being totally valid.

1.7. Part G

The mass column density as a function of pressure is shown in Figure 7. The pressure increases linearly with mass column density which makes sense because $P_{tot} = m \times g$. The slope of this line reveals the value of g assumed in the model, $g \approx 27396.52 \text{ cm/s}^2$ corresponding to $\log(g) = 4.43$.

1.8. Part H

The molecular mass fraction of Hydrogen and Helium is shown in Figure 8. I calculated the mass density based off the number density given in the table. For Hydrogen, $\rho_H = n_H \mu M_H$, where M_H is the mass of Hydrogen and $\mu=1.0$ is the mean molecular weight. Then, to compute the mass density of Helium I used the given Hydrogen-to-Helium ratios ($N(\text{He})/N(\text{H}) = 0.1$ and $m(\text{He})/m(\text{H}) = 3.97$) and followed a similar prescription.

The ratio of molecular mass density to total mass density reveals that the mean molecular mass fractions in the Sun are as follows; 71.4% Hydrogen and 28.3% Helium. Note that the values for Hydrogen and Helium do not add up

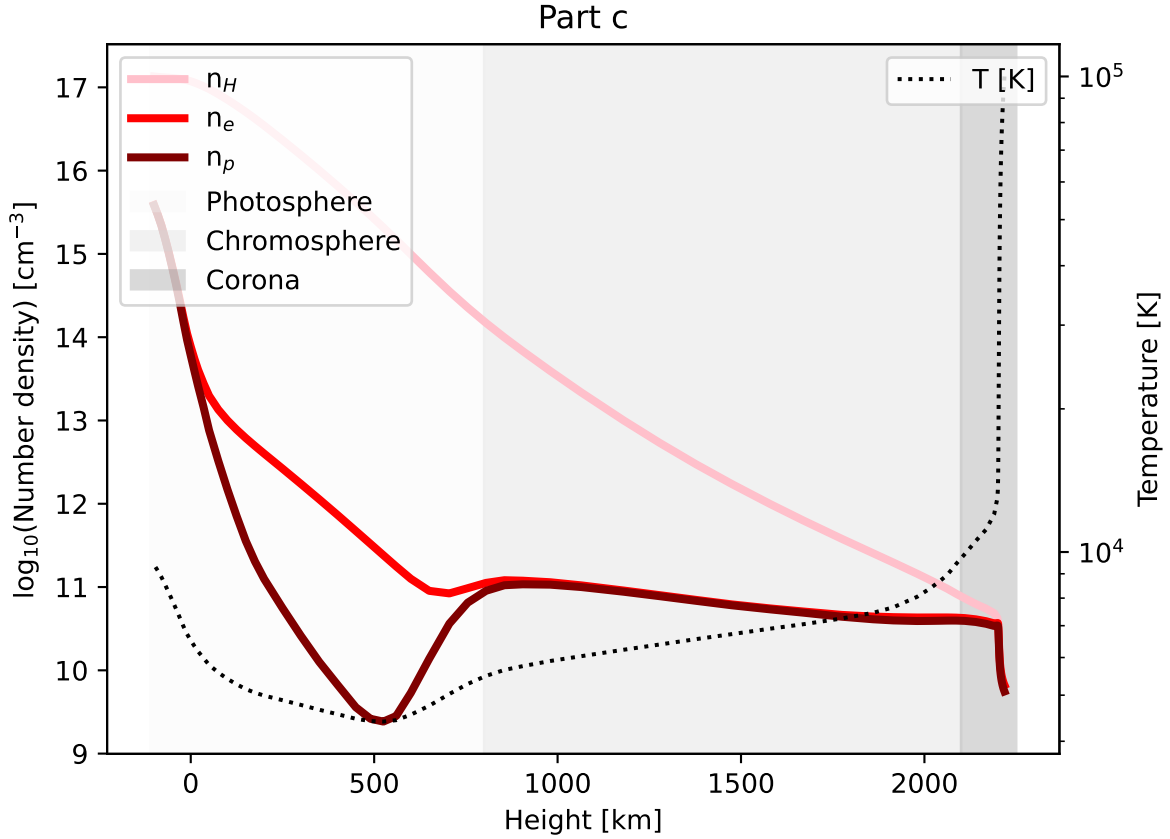


Figure 3. log(Number density) vs. Height. The number density of Hydrogen (pink), electrons (red), and protons (maroon) are shown, corresponding to the left axis. The dotted line, corresponding to the right axis, is the temperature profile of the Sun from 1.1. As determined by the temperature profiles, the shaded regions represent the photosphere, the chromosphere, and the corona respectively.

exactly to 100% because of the small amount of metals also present in the atmosphere. The molecular mass fractions of each element are relatively constant at all heights because complete mixing was assumed in the model.

Based on the Hydrogen and Helium mass fractions I was able to calculate the average molecular mass fraction of metals since,

$$\langle \rho_H / \rho_{tot} \rangle + \langle \rho_{He} / \rho_{tot} \rangle + \langle \rho_{metals} / \rho_{tot} \rangle = 100\% \quad (4)$$

I estimate the average mass fraction of metals in the Sun to be 0.2%.

1.9. Part I

The turbulent velocity profile of the Solar atmosphere is shown in Figure 9. The turbulent velocity is the smallest in the photosphere, ≈ 2 km/s, it then increases steadily in the chromosphere to ≈ 8 km/s. The turbulent velocity shoots up to ≈ 12 km/s in the corona at the very top of the atmosphere. This reveals that turbulence increases as you go outwards from the "surface" of the star.

Turbulent velocity is related to turbulent pressure,

$$P_{turb} = \frac{1}{2} \rho v_{turb}^2. \quad (5)$$

The resulting turbulent pressure from Equation 5 is shown in Figure 10. In all regions of the atmosphere, the gas pressure is dominating and turbulent pressure is more that 1 order of magnitude smaller. The small contribution of turbulent pressure is needed to achieve the total pressure in the atmosphere.

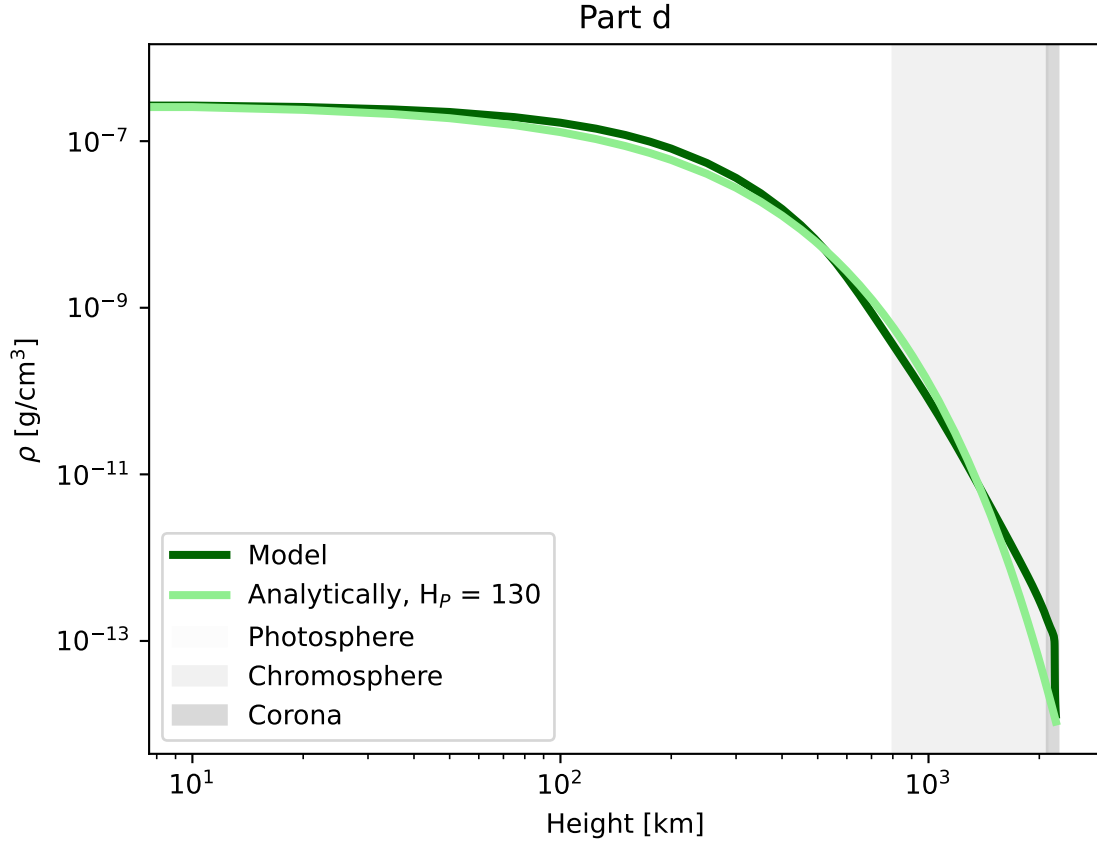


Figure 4. Density vs. Height. The stratification of density in the Solar atmosphere (dark green). Also plotted, in light green, is the analytical solution to $\rho = \rho_0 e^{-h/H_\rho}$; Where $\rho_0 = \rho(h = 0)$, and I found the density scale height $H_\rho \approx 130$ km is a good match to the model. As determined by the temperature profiles, the shaded regions represent the photosphere, the chromosphere, and the corona respectively.

2. PART II

In this section I begin to "build-up" the model atmosphere.

2.1. Part K

Astrophysical flux (F_λ) and emergent intensity (I_λ) as a function of wavelength are shown in Figure 11. The shape of the emergent intensity curve is familiar as it looks almost like a blackbody. This figure reveals that the emergent intensity peaks at $\lambda = 0.41 \mu\text{m}$.

2.2. Part L

To proceed with modeling the Solar spectrum, I will assume a plane-parallel atmosphere that consists of two parts: (i) a semi-infinite lower part at temperature T_L that lies below (ii) an upper part at temperature T_U . I will assume local thermodynamic equilibrium such that a source function equals the Planck function, $S_\lambda = B_\lambda(T)$. This is also known as a Schuster-Schwarzschild model.

I will now analytically solve the radiative transfer equation of the previously described model atmosphere to derive the equation for emergent intensity. To begin, the equation of radiative transfer is

$$\frac{dI}{d\tau} = S_\lambda - I_\lambda \quad (6)$$

multiply both sides by the attenuation factor, $e^{-\tau}$,

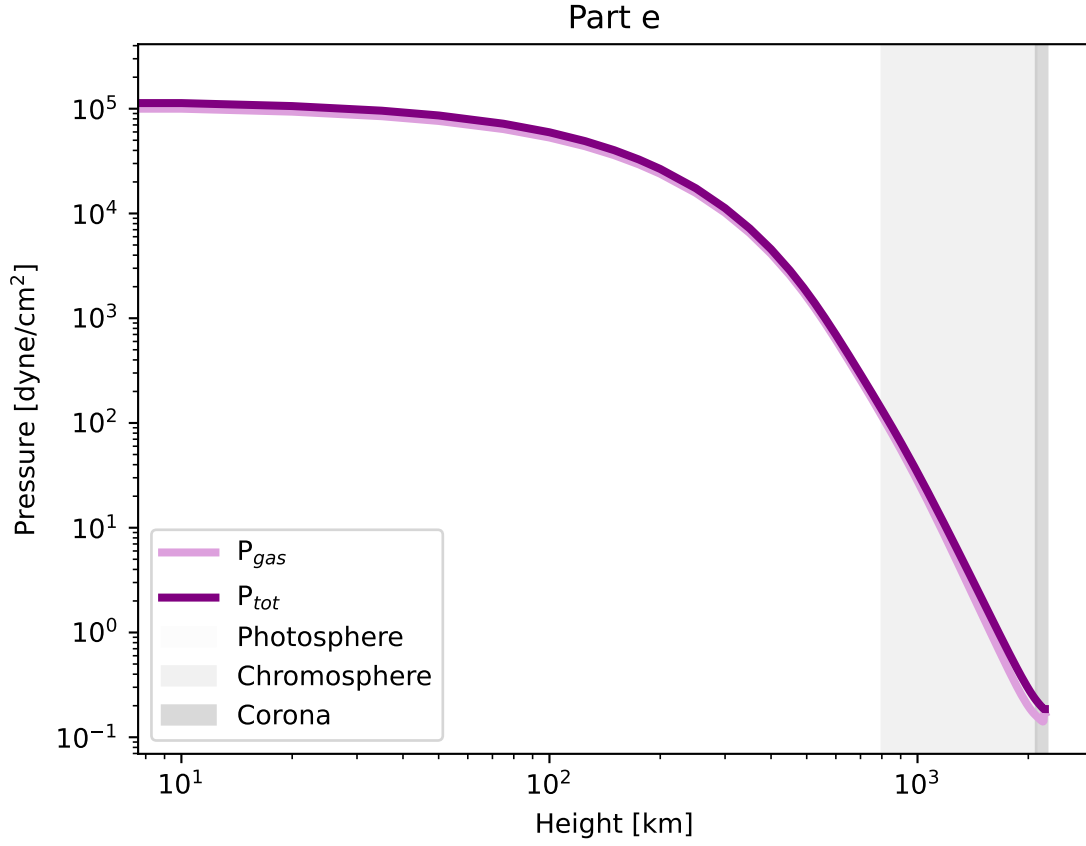


Figure 5. Pressure vs. Height. Shown in the figure is the total pressure from the model (purple) as well as the gas pressure calculated from the ideal gas law (light purple). Overall, P_{gas} is a good match to P_{tot} , with small deviations near the surface and larger deviations at the very top of the chromosphere and the corona. As determined by the temperature profiles, the shaded regions represent the photosphere, the chromosphere, and the corona respectively.

$$\frac{dI}{d\tau} e^{-\tau_\lambda} = (S_\lambda - I_\lambda) e^{-\tau_\lambda} \quad (7)$$

applying integration by parts leads to,

$$I_\lambda = I_\lambda(0) e^{-\tau_\lambda} + \int_0^\tau S_\lambda e^{-\tau_\lambda} d\tau_\lambda \quad (8)$$

now take the integral,

$$I_\lambda = I_\lambda(0) e^{-\tau_\lambda} + S_\lambda (1 - e^{-\tau_\lambda}) \quad (9)$$

And from the set-up of the model I know that $I_\lambda(0) = B_\lambda(T_L)$ and $S_\lambda = B_\lambda(T_U)$, where $B_\lambda(T)$ is the Planck function. Therefore,

$$I_\lambda = B_\lambda(T_L) e^{-\tau_\lambda} + B_\lambda(T_U) (1 - e^{-\tau_\lambda}) \quad (10)$$

2.3. Part M

The Planck function describes the intensity of a blackbody; most stars, including the Sun, radiate like a blackbody. The general form of the Planck function is:

$$B_\lambda(T) = \frac{2hc^2}{\lambda^5} \frac{1}{e^{\frac{hc}{\lambda k_B T}} - 1} \quad (11)$$

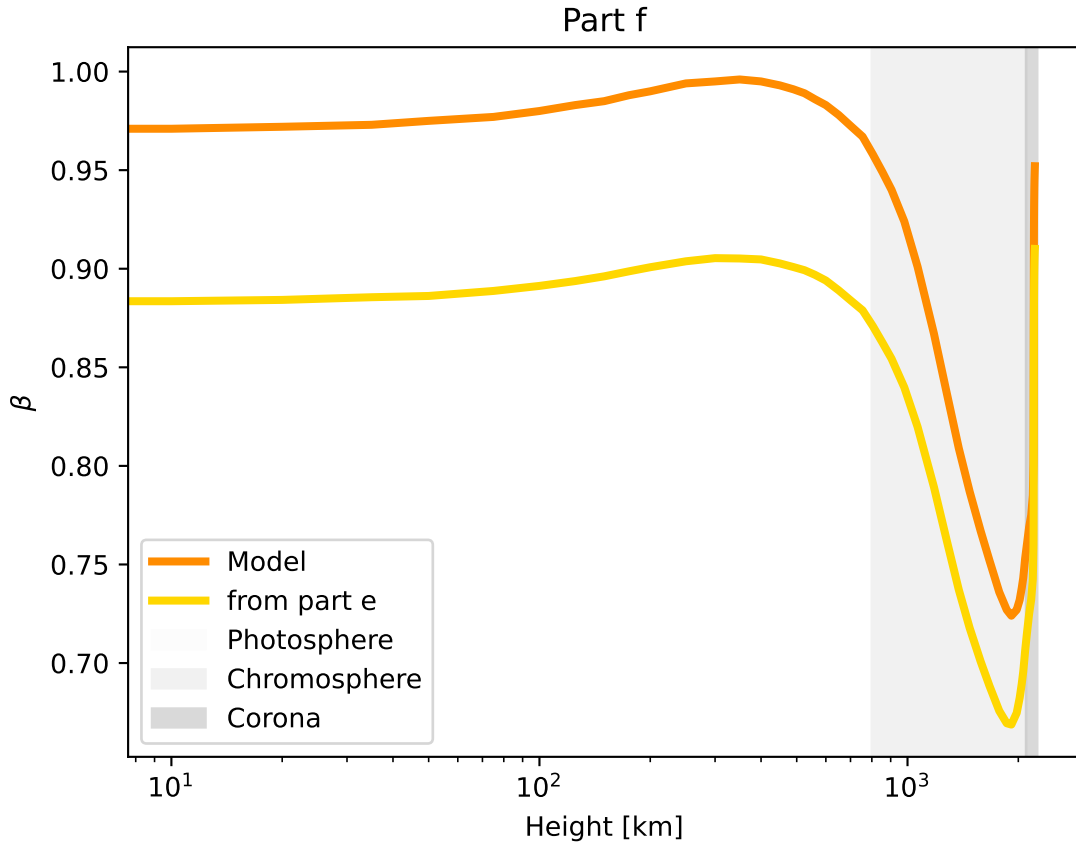


Figure 6. Beta vs. Height. $\beta = \frac{P_{gas}}{P_{tot}}$ from the realistic model (orange) and β calculated using my P_{gas} from Section 1.5. As determined by the temperature profiles, the shaded regions represent the photosphere, the chromosphere, and the corona respectively.

For example, Figure 12 shows the blackbody spectrum for temperatures relevant to stellar atmospheres (4000 K, 5000 K, 6000 K, and 7000 K). Importantly, the hottest object is brightest at all wavelengths.

2.4. Part N

The Solar spectrum is almost a perfect blackbody spectrum as shown in Figure 13. I found that a temperature of 6200 K produced a blackbody spectrum that is a good fit to the data.

2.5. Part O

In order to model spectral lines it is essential to know the abundance of a given element, as well as the distribution of electron energy levels. The Boltzmann equation is helpful here, as it described the level population for bound electrons. The Boltzmann equation is:

$$\frac{n_2}{n_1} = \frac{g_2}{g_1} e^{-(E_2 - E_1)/(kT)} \quad (12)$$

where g_1 and g_2 are the statistical weights for level 1 and level 2 respectively. Similarly, E_1 and E_2 are the energy of the levels. Also, k is the Boltzmann constant and T is temperature.

Another useful equation is the Saha equation, which describes the level populations for ionized states:

$$\frac{n_+}{n_i} = \frac{2kT}{P_e} \frac{U_{II}}{U_I} \left(\frac{2\pi m_e kT}{h^2} \right)^{2/3} e^{\chi_i/kT} \quad (13)$$

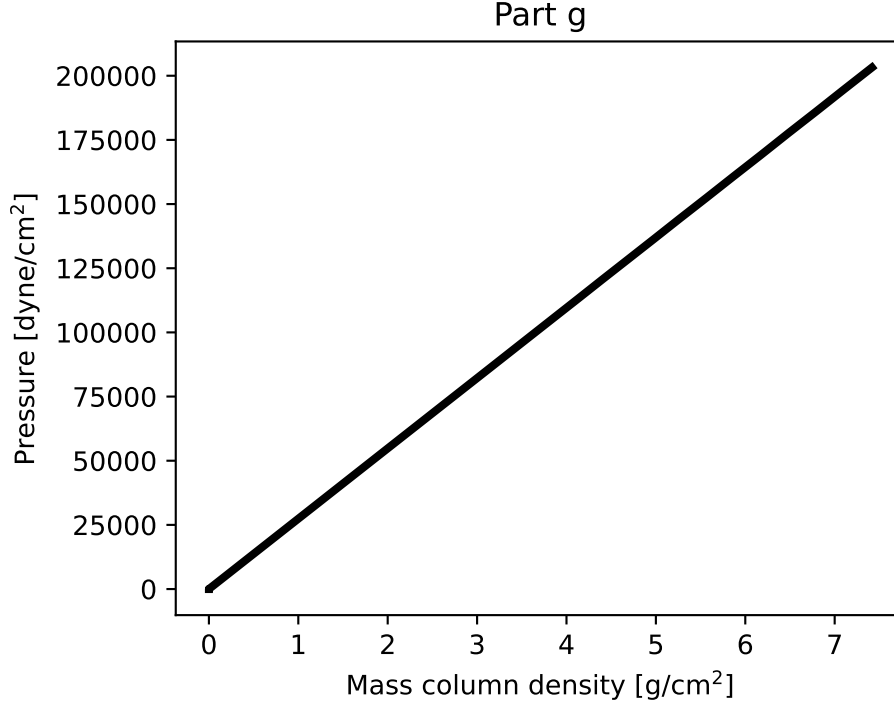


Figure 7. Pressure vs. Mass Column Density. Pressure increases linearly with mass column density since $P_{tot} = m \times g$. The slope of this line reveals the value of g assumed in the model, so $g \approx 27396.52 \text{ cm/s}^2$.

| wavelength (Å) | f_{lu} | g_l | g_u | E_l (eV) | E_u (eV) |
|----------------|----------|-------|-------|------------|------------|
| 5889.95 | 0.641 | 2 | 4 | 0.0000 | 2.1044 |

Table 1. Atomic level and transition properties of the Na I D1 line. Also relevant is the ionization energy of Na which is $\chi = 8.23 \times 10^{-12} \text{ erg}$ and the partition functions: $U_{NaI} = 1$ and $U_{NaII} = 6$.

where P_e is electron pressure, assumed to be 200 dyne cm^{-2} for constant electron pressure. U_I and U_{II} are the partition function for the two levels. And χ_i is the ionization energy of the electron.

Let's take the "famous" Na D1 line for example. The relevant atomic parameters for Na D1 are shown in Table 1, given to me for this assignment. Also given to me were the partition functions: $U_{NaI} = 1$ and $U_{NaII} = 6$. Also relevant is the ionization energy of Na which is $\chi = 8.23 \times 10^{-12} \text{ erg}$.

Plugging in the values from Table 1 into the Boltzmann equation (Eqn 12), and assuming $T = 6000 \text{ K}$, results in $\frac{n_2}{n_1} = 0.0342$. And the Saha equation (Eqn 13) results in $\frac{n_+}{n_i} = 23394.47$. Also helpful is the Saha-Boltzmann distribution, which is a combination of the two results:

$$\frac{n_l}{n_E} = \frac{1}{n_2/n_1 + 1} \frac{1}{n_+/n_i + 1} \quad (14)$$

where n_2/n_1 is the result of the Boltzmann equation and n_+/n_i is the result of the Saha equation. Plugging in the values from Table 1 into equation 14 I found $\frac{n_l}{n_E} = 4.13 \times 10^{-5}$. For further visualization, the result of the Boltzmann and Saha equations as a function of temperature are shown in Figure 14.

2.6. Part P

Recall the derived equation of radiative transfer for the model atmosphere. I will now begin to explain how to express the optical depth term, τ_λ . The optical depth can be expressed with a linear extinction coefficient α_λ , i.e. $\tau_\lambda(h) = \int_\infty^h \alpha_\lambda dl$. The equation for the linear extinction coefficient is:

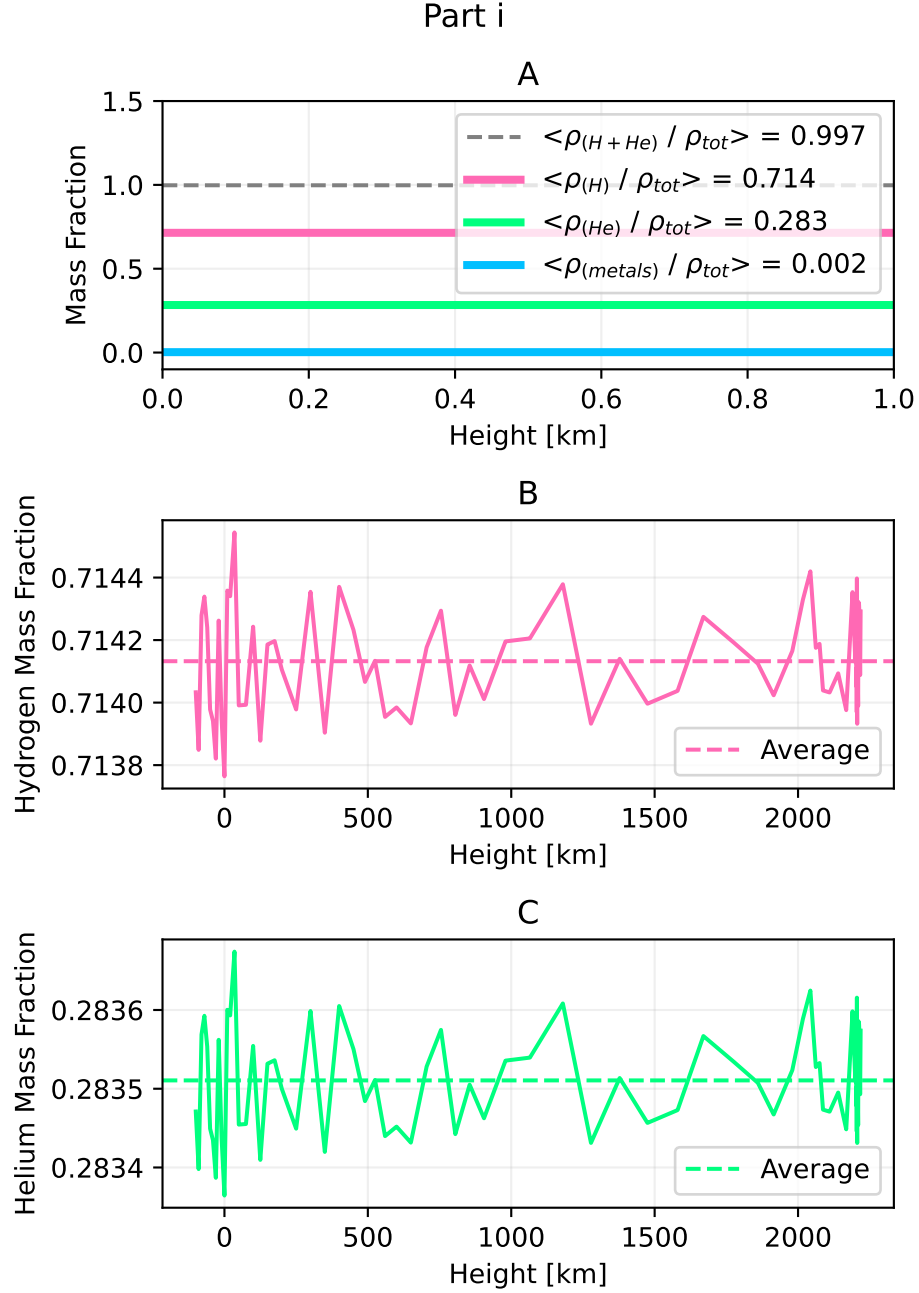


Figure 8. Mass Fraction vs. Height. Top panel: Average molecular mass fraction of Hydrogen (pink), Helium (green), and metals (blue) in the Sun assuming complete mixing. The grey dashed line represents the sum of the molecular mass fraction of Hydrogen and Helium, note that the sum is slightly less than 1.0. Middle panel: Zoom-in of top panel showing the molecular mass fraction of Hydrogen in the Sun as well as the average (dashed line). Bottom panel: Zoom-in of top panel showing the molecular mass fraction of Helium in the Sun as well as the average (dashed line). The molecular mass fractions of each element are relatively constant throughout the atmosphere because complete mixing was assumed.

$$\alpha_{\lambda_0} = \frac{\pi e^2}{m_e c} \frac{\lambda_0^2}{c} \frac{n_l}{n_E} n_H A_E f_{lu} (1 - e^{-hc/\lambda_0 kT}) \quad (15)$$

where e is the electron charge, m_e is the mass of the electron, c is the speed of light. And λ_0 is the wavelength of the line, n_l/n_E is the result of the Saha-Boltzmann distribution (Eqn 14, see section 2.5), A_E is the abundance of element

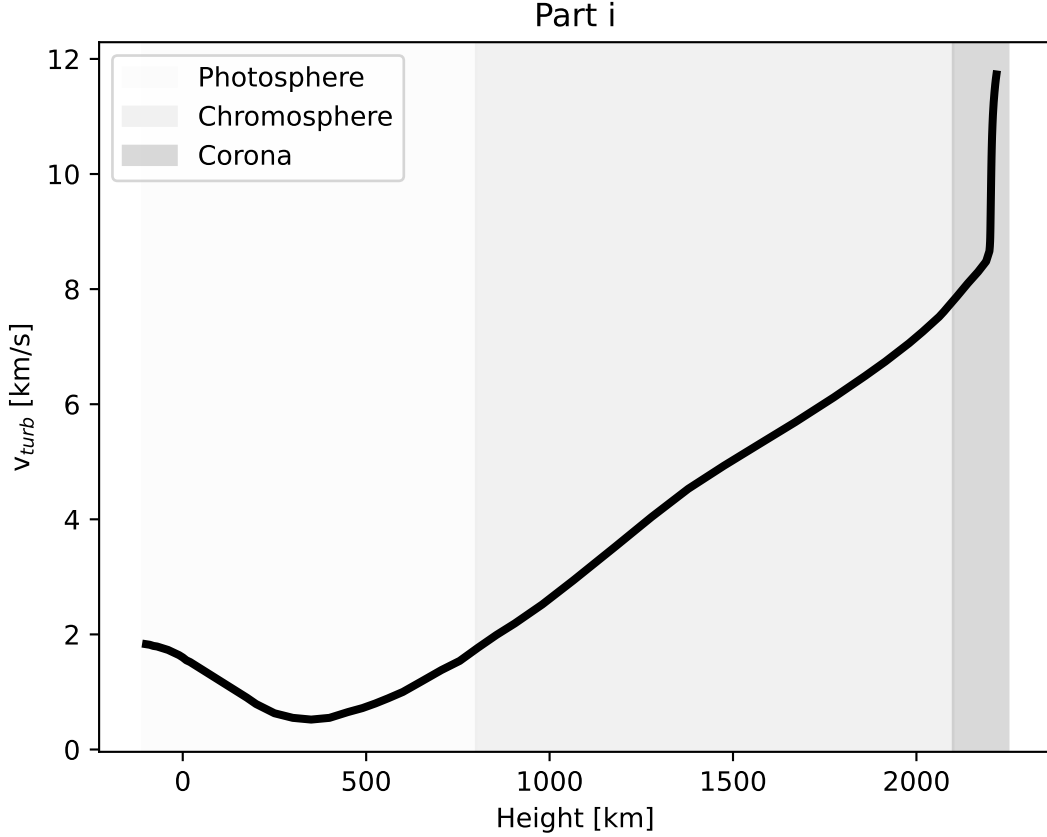


Figure 9. Turbulent Velocity vs. Height. The turbulent velocity profile of the solar atmosphere. As determined by the temperature profiles, the shaded regions represent the photosphere, the chromosphere, and the corona respectively.

"E" ($A_{Na} = 1.8 \times 10^{-6}$), and f_{lu} is the oscillator strength. In the next subsection, I will calculate α_{λ_0} for the Solar atmosphere Na D1 line.

2.7. Part Q

To model the extinction coefficient of the Solar atmosphere I must refer back to some of the data from Part I. Specifically, n_H is the number density of Hydrogen which I obtained from the data from Part I. I will also use the temperature data from Subsection 1.1.

Going back to the example of the Na D1 line, the resulting extinction coefficient, α_λ , as a function of temperature is shown in Figure 15. I would expect to see Na D1 absorption lines for temperatures ranging from 1000 K - 10000 K, where α_{λ_0} is largest. The extinction coefficient is largest at temperatures less than 10000 K, corresponding to the photosphere and chromosphere regions of the star. Indicating that the "surface" of the star may be easiest to probe.

2.8. Part R

The total prescription for optical depth is $\tau_\lambda = \tau_{\lambda_0} \phi(\lambda - \lambda_0)$. Where the $\phi(\lambda - \lambda_0)$ component describes the "broadening profile" of the line, typically a Lorentzian form. Various effects cause the broadening, but it can generally be well described by the Voigt profile:

$$\phi(\lambda - \lambda_0) = \frac{1}{\sqrt{\pi} \Delta \lambda_D} V(a, u) \quad (16)$$

where $\Delta \lambda_0$ is the Doppler width, $\Delta \lambda_0 = (\lambda_0/c) \sqrt{2kT/m + v_{turb}^2}$. And the Voigt function $V(a, u)$ is defined as a convolution but can be approximated numerically. I use the dimensionless $u = \frac{\lambda - \lambda_0}{\Delta \lambda_D}$ in place of the wavelength scale for simplicity. Here, a is called the "impact parameter" and depends on the specifics of the broadening mechanism.

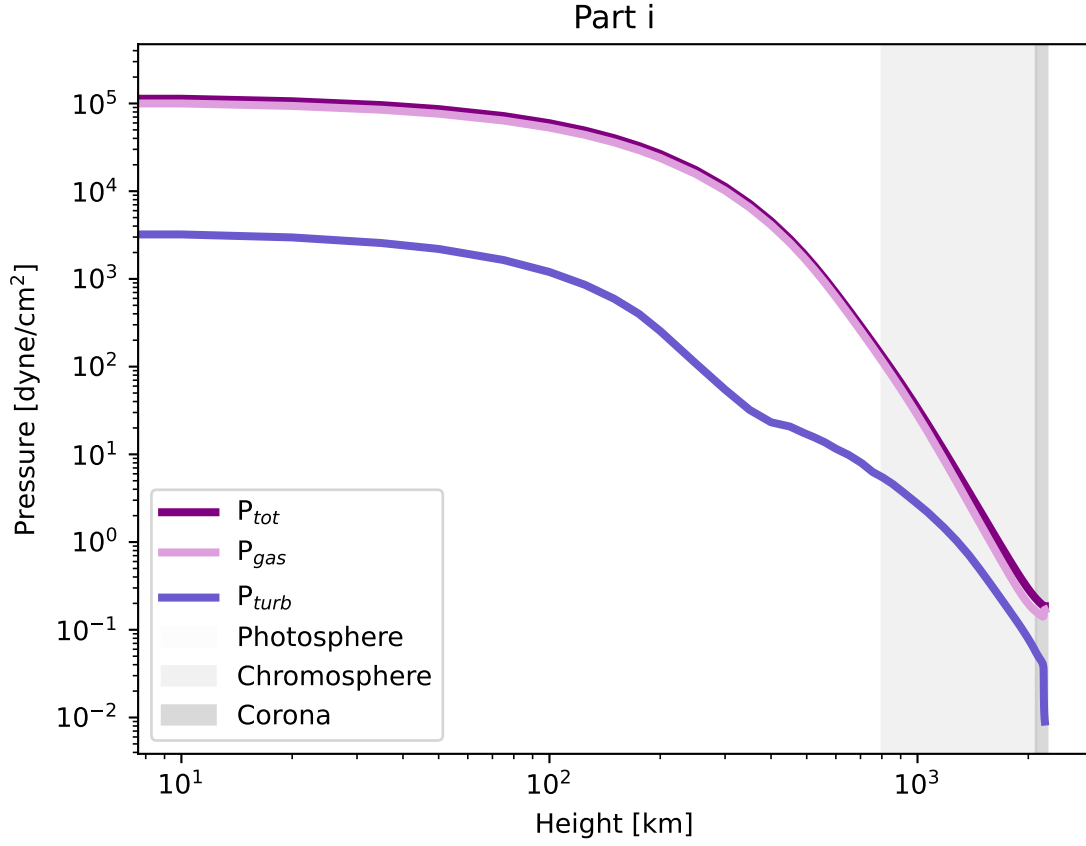


Figure 10. The total pressure (purple), gas pressure from part 1.5 (light purple), and turbulent pressure calculated from Equation 5 (blue). As determined by the temperature profiles, the shaded regions represent the photosphere, the chromosphere, and the corona respectively.

Some examples of the Voigt function for different impact parameters are shown in Figure 16. Noticeably, the Voigt profile for $a = 1.0$ is much broader than for smaller values of a . Additionally, the wings of the $a = 1.0$ Voigt profile are shifted upward compared to smaller values of a . The profile with $a = 0.001$ has the tallest peak, and the peak decreases for larger values of a . Another way of summarizing this is, for higher values of a , the Voigt profile both broadens horizontally and shrinks vertically.

3. PART III

In this section, the culmination of the previous two parts finally renders a model absorption line.

3.1. Part S

Recall the equation for emergent intensity derived earlier:

$$I_{\lambda} = B_{\lambda}(T_L)e^{-\tau_{\lambda}} + B_{\lambda}(T_U)(1 - e^{-\tau_{\lambda}}) \quad (17)$$

Now we have everything we need to calculate the optical depth, τ_{λ} , and correspondingly the intensity, I_{λ} , as a function of height in the model atmosphere. Functionally I evaluate, $\tau_{\lambda}(H) = -\alpha_{\lambda}H\phi(\lambda - \lambda_0)$. Where α_{λ} is the extinction coefficient from part 2.7, and $\phi(\lambda - \lambda_0)$ is the Voigt profile described in part 2.8. The product of these two components (assuming the impact parameter, $a = 0.1$, and $\lambda = 5000 \text{ \AA}$) with height results in the optical depth shown in Figure 17.

3.2. Part T

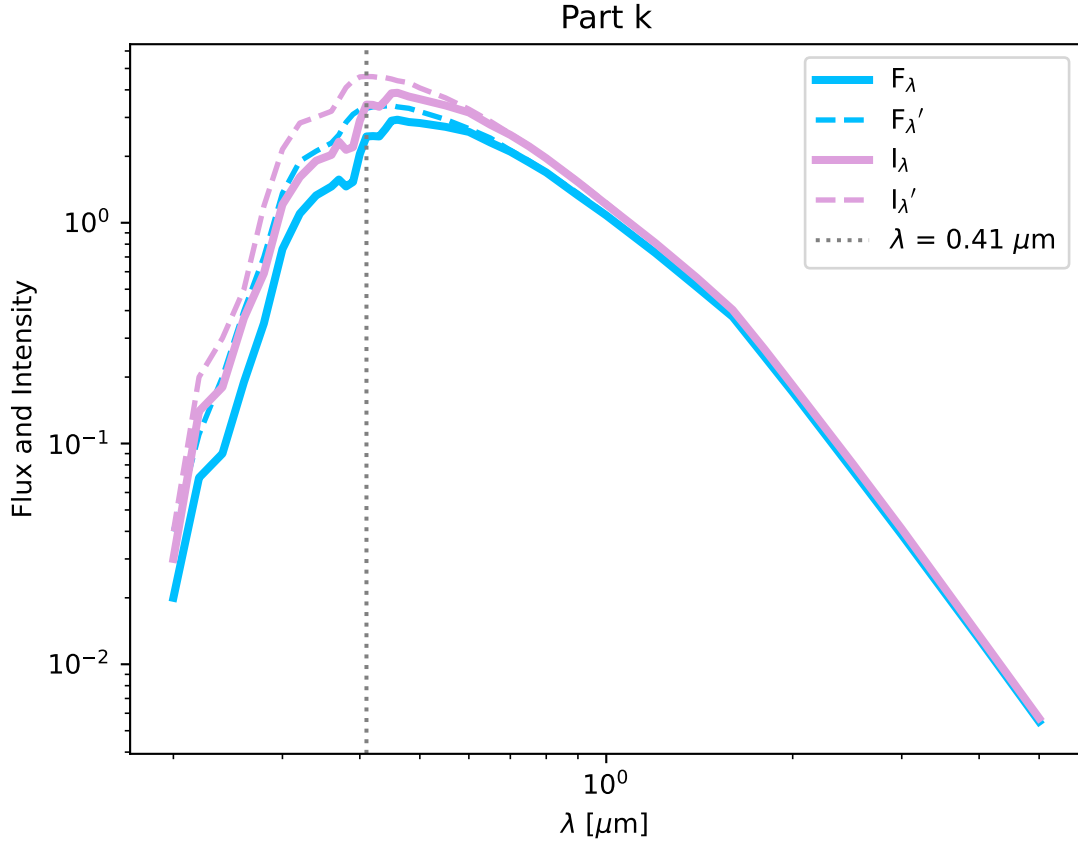


Figure 11. Astrophysical flux (F_λ , in blue) and emergent intensity (I_λ , in green) are shown as a function of wavelength. Also shown, as dashed curves, are the continuum flux and continuum emergent intensity. The emergent intensity peaks at $\lambda = 0.41 \mu\text{m}$, highlighted by the dotted grey line.

The resulting model absorption line for Na D1 in the Solar atmosphere is shown in Figure 18. Note that the intensity is in terms of the dimensionless quantity u (not λ), the intensity peaks at $u=0.0$ by convention. Noticeably, the line does have some broadening as a result of the contribution from the Voigt profile. The peak intensity is on the order of $10^{-12} \text{ ergs}^{-1} \text{ cm}^{-2} \text{ Hz}^{-1} \text{ sr}^{-1}$, which is relatively small compared to the overall intensity of the Sun.

3.3. Part U

A direct comparison between the model and observational Solar spectrum is not exactly straightforward. First of all, the model intensity is in terms of the dimensionless u , whereas the data is in terms of wavelength λ . At this time the conversion between u and λ is not clear. Secondly, after a deeper look at the provided observational Solar spectrum I could not find the Na doublet anywhere around 5000 \AA . Even after taking the residual of the continuum emission with the total emission, no doublet appeared. Prior knowledge rules out the possibility that there may just be no Na in the Solar atmosphere. So, this makes me think that the data may not have been sensitive enough to recover the faint Na doublet.

That being said, my attempt at a comparison between the model and data is shown in Figure 19. In the figure, Panel A is the result when I subtract the model absorption line from the model blackbody function. The absorption line is too faint to actually see in the spectrum, but taking the residual of the model blackbody and the model absorption line reveals the feature right around $u = 0.0004$ (Panel B). Panel C is the Solar spectrum from the data including spectral lines, the same as in Figure 11. And the residual of the continuum emission and the total intensity from the data is shown in Panel D. I was surprised that no Na doublet appeared $0.5 \mu\text{m}$ even in the residual plot. While this is a good start, further work is necessary to properly compare the model to data.

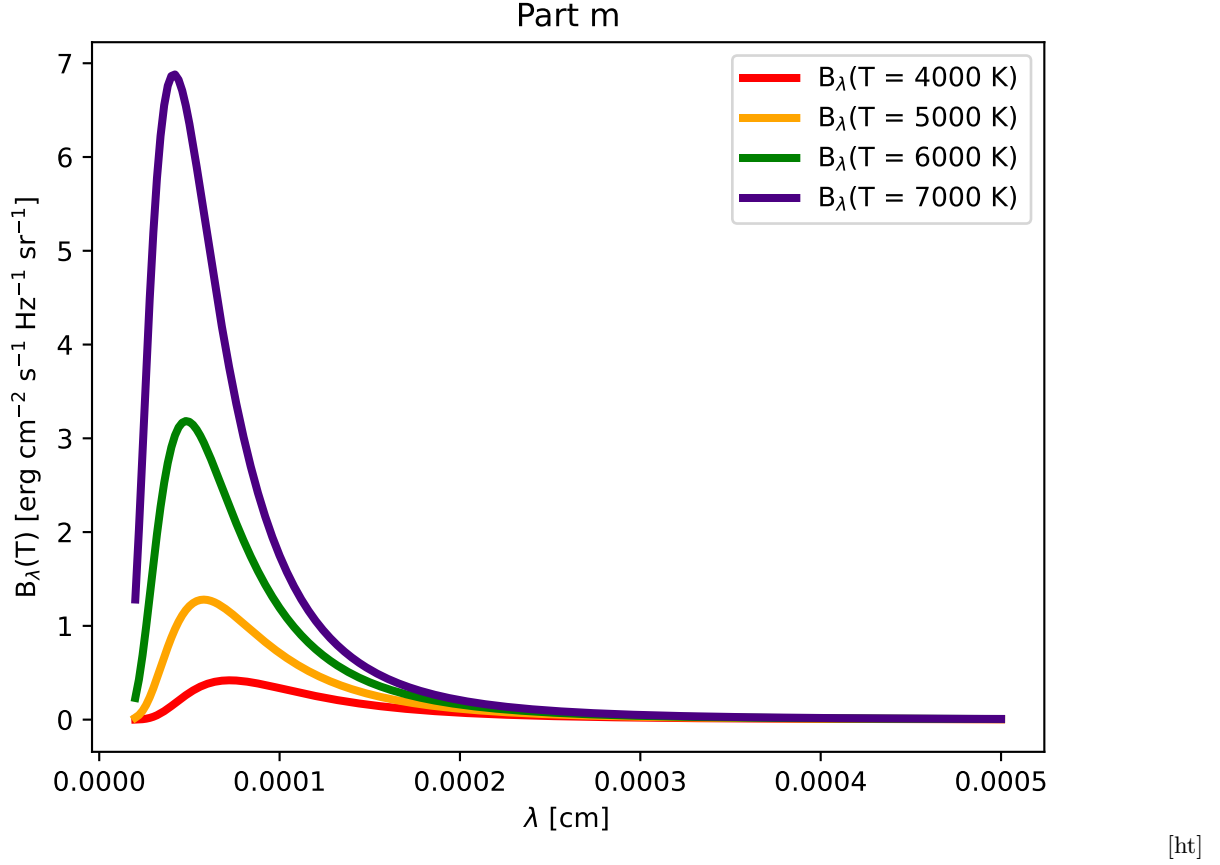


Figure 12. Planck Function. The resulting Planck function, B_λ , for different temperatures relevant to stellar atmospheres: 4000 K, 5000 K, 6000 K, and 7000 K. The hottest object is brightest at all wavelengths.

Facilities:

Software: astropy (Astropy Collaboration et al. 2013, 2018), Cloudy (Ferland et al. 2013), Source Extractor (Bertin & Arnouts 1996)

REFERENCES

- | | |
|--|--|
| <p>Allen, C. W. 1976. https://www.osti.gov/biblio/4323708</p> <p>Astropy Collaboration, Robitaille, T. P., Tollerud, E. J., et al. 2013, A&A, 558, A33, doi: 10.1051/0004-6361/201322068</p> <p>Astropy Collaboration, Price-Whelan, A. M., Sipőcz, B. M., et al. 2018, AJ, 156, 123, doi: 10.3847/1538-3881/aabc4f</p> | <p>Bertin, E., & Arnouts, S. 1996, A&AS, 117, 393, doi: 10.1051/aas:1996164</p> <p>Ferland, G. J., Porter, R. L., van Hoof, P. A. M., et al. 2013, RMxAA, 49, 137. https://arxiv.org/abs/1302.4485</p> <p>Fontenla, J. M., Avrett, E. H., & Loeser, R. 1993, ApJ, 406, 319, doi: 10.1086/172443</p> |
|--|--|

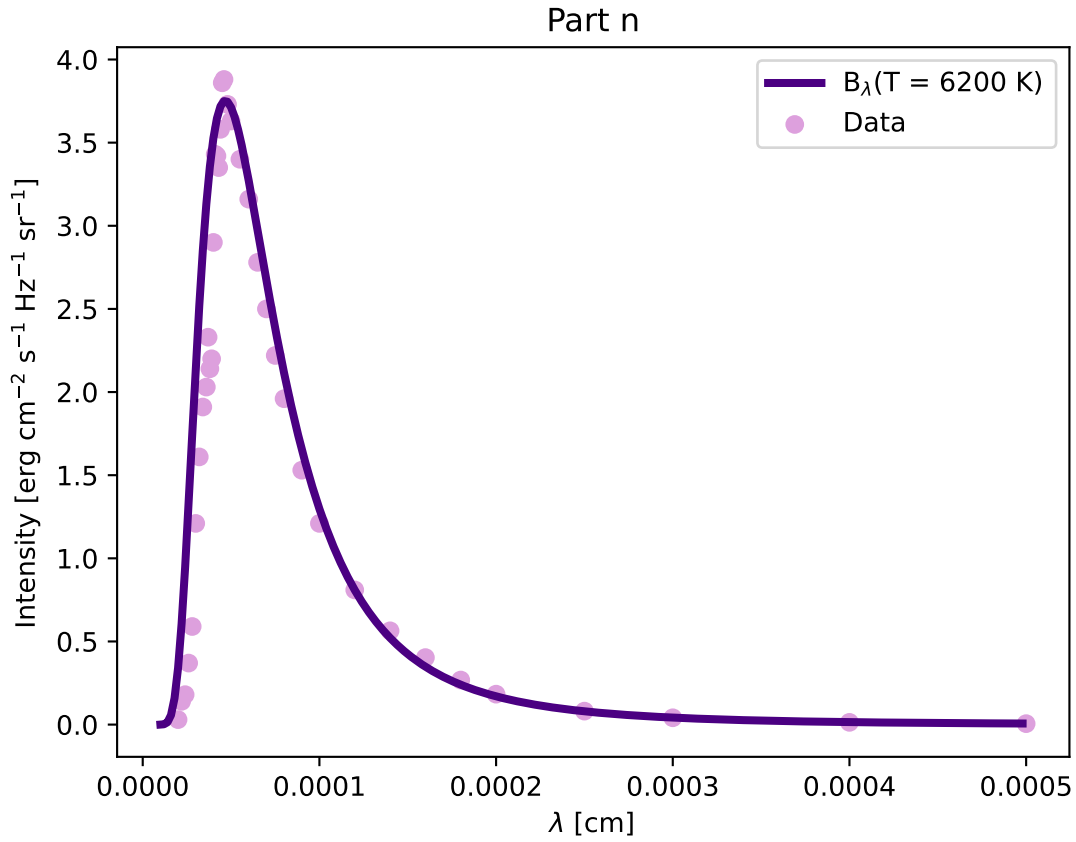


Figure 13. The blackbody spectrum of a 6200 K object is a good fit to the Solar intensity data. This is slightly hotter than the reported temperature of the Sun which is closer to 5772 K.

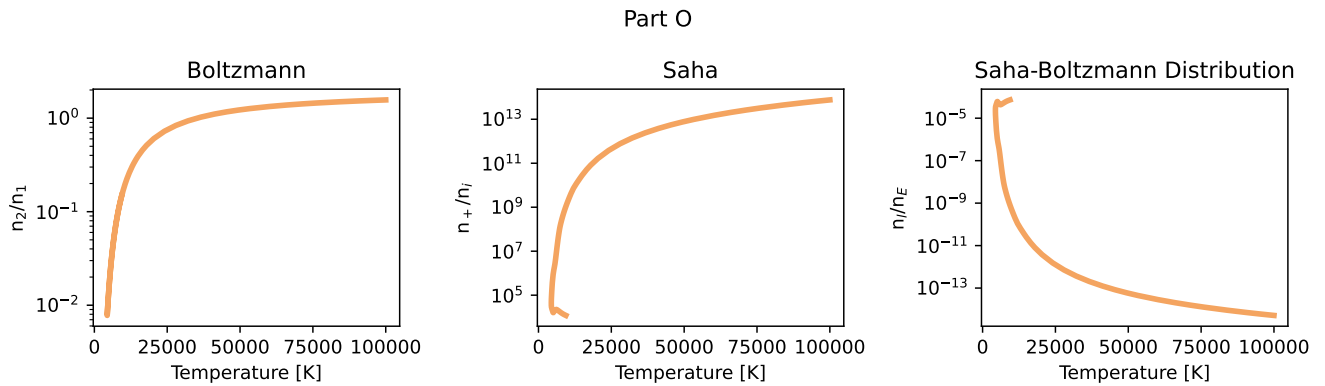


Figure 14. Boltzmann and Saha Level Populations. Left panel: Result of the Boltzmann equation (Equation 12) as a function of temperature in the Solar atmosphere. Middle panel: Result of the Saha equation (Equation 13) a function of temperature in the Solar atmosphere. Right panel: The Saha-Boltzmann distribution (Equation 14) a function of temperature in the Solar atmosphere.

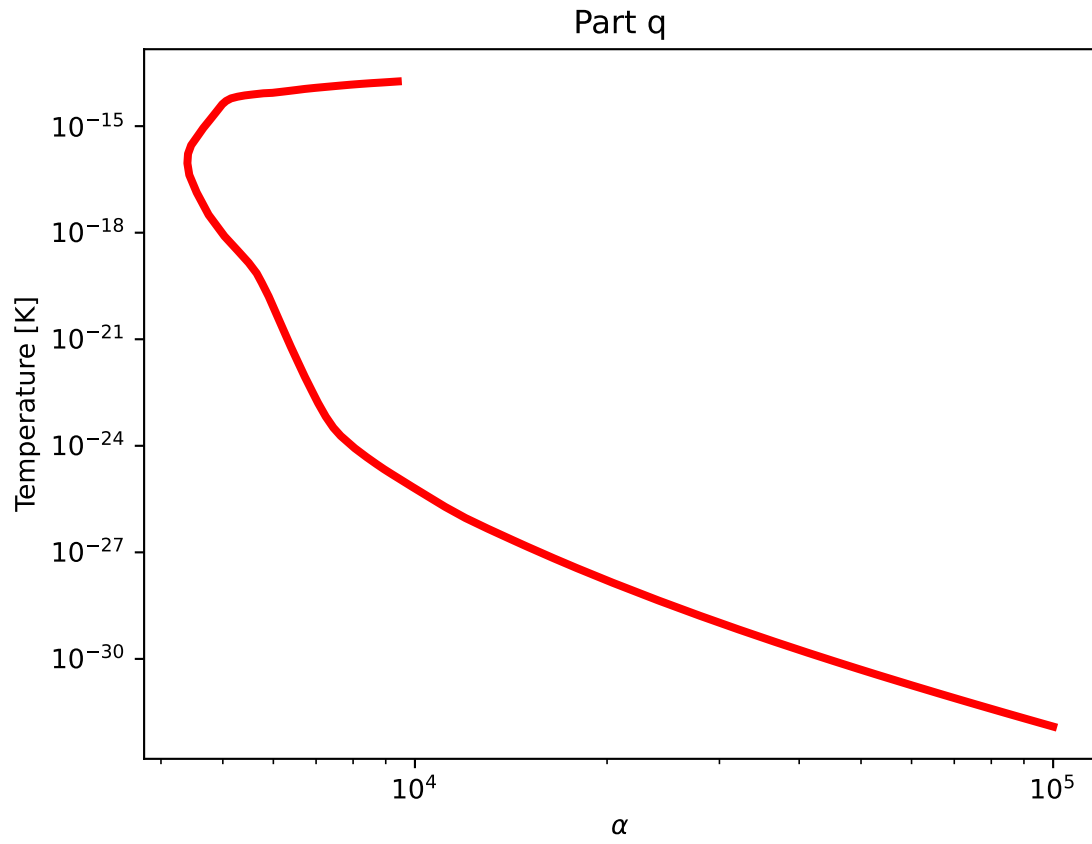


Figure 15. Extinction coefficient vs. temperature. The extinction coefficient for the Na D1 line of the model Solar atmosphere. The extinction coefficient, $\alpha_{\lambda 0}$, increases as temperature decreases. I would expect to see Na D1 absorption lines for temperatures ranging from 1000 K - 10000 K, where $\alpha_{\lambda 0}$ is largest.

Part r

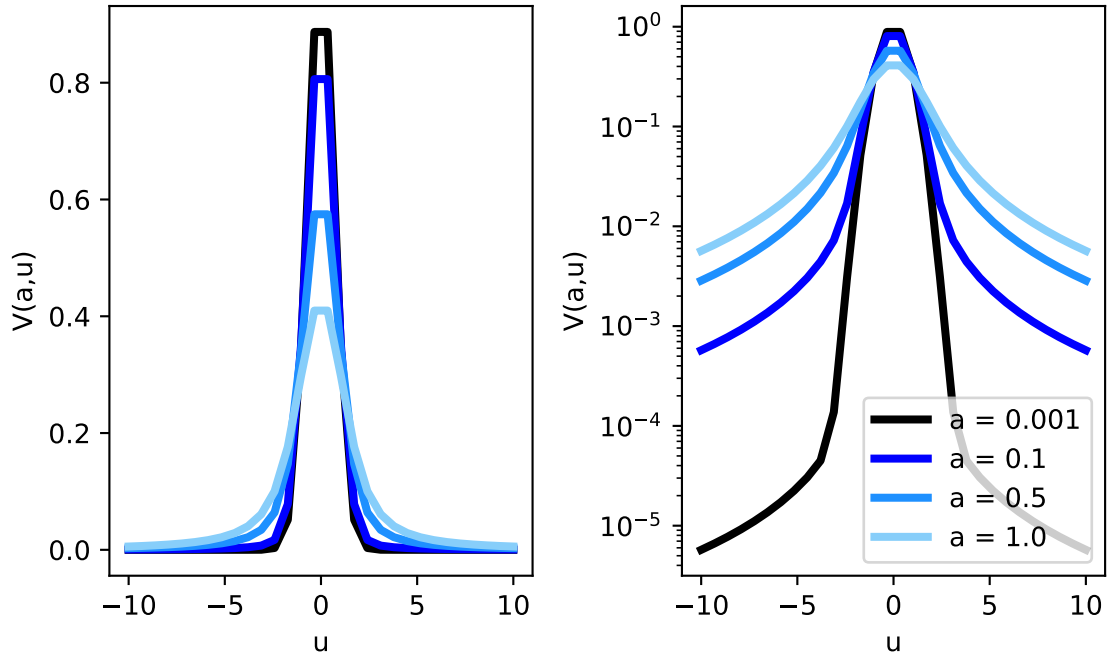


Figure 16. Voigt Function. The Voigt function, $V(a, u)$, for various values of the parameter a . The right panel is the same as the left panel but with the y-axis in log-scale. Noticeably, the Voigt profile for $a = 1.0$ is much broader than for smaller values of a . Additionally, the wings of the $a = 1.0$ Voigt profile are shifted upward compared to smaller values of a . The profile with $a = 0.001$ has the tallest peak, and the peak decreases for larger values of a . Another way of summarizing this is, for higher values of a , the Voigt profile both broadens horizontally and shrinks vertically.

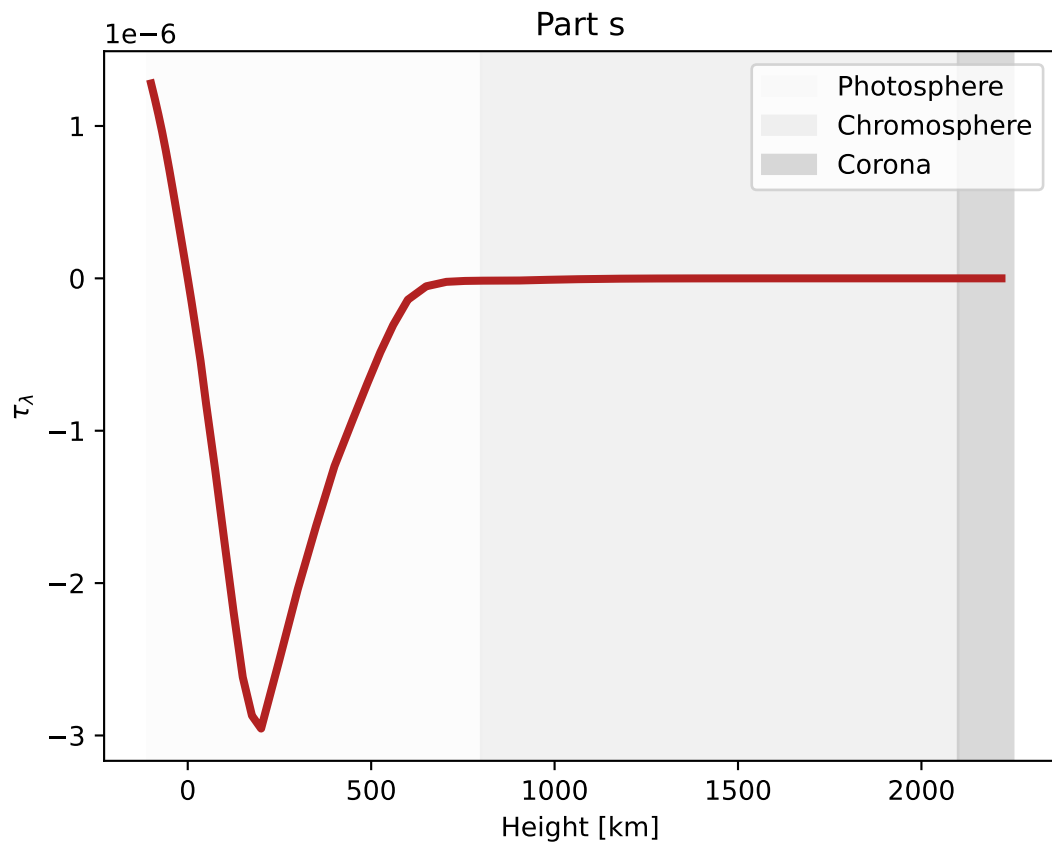


Figure 17. Optical Depth Optical depth for the NaD1 line in the model Solar atmosphere. As determined by the temperature profiles, the shaded regions represent the photosphere, the chromosphere, and the corona respectively.

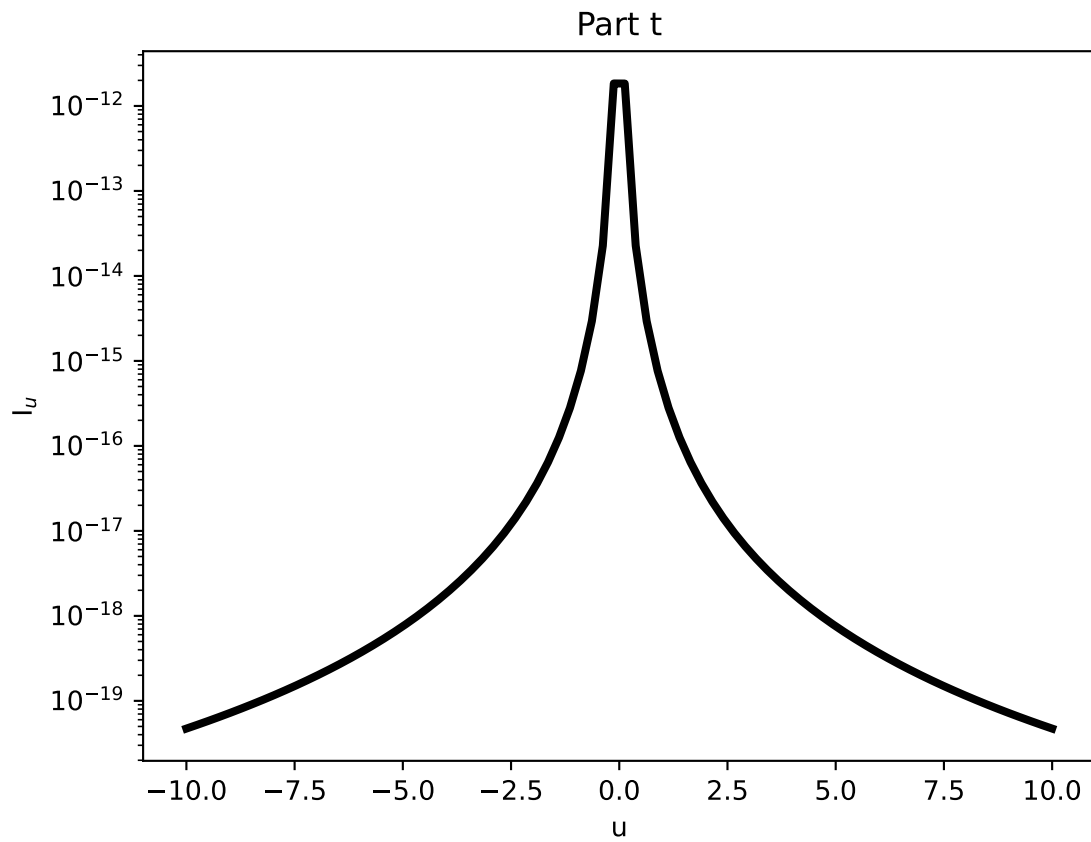


Figure 18. Model Absorption Line The model absorption line for Na D1 in the Solar atmosphere as a function of the dimensionless wavelength quantity u . The peak intensity is on the order of $10^{-12} \text{ ergs}^{-1} \text{ cm}^{-2} \text{ Hz}^{-1} \text{ sr}^{-1}$, which is relatively small compared to the overall intensity of the Sun.

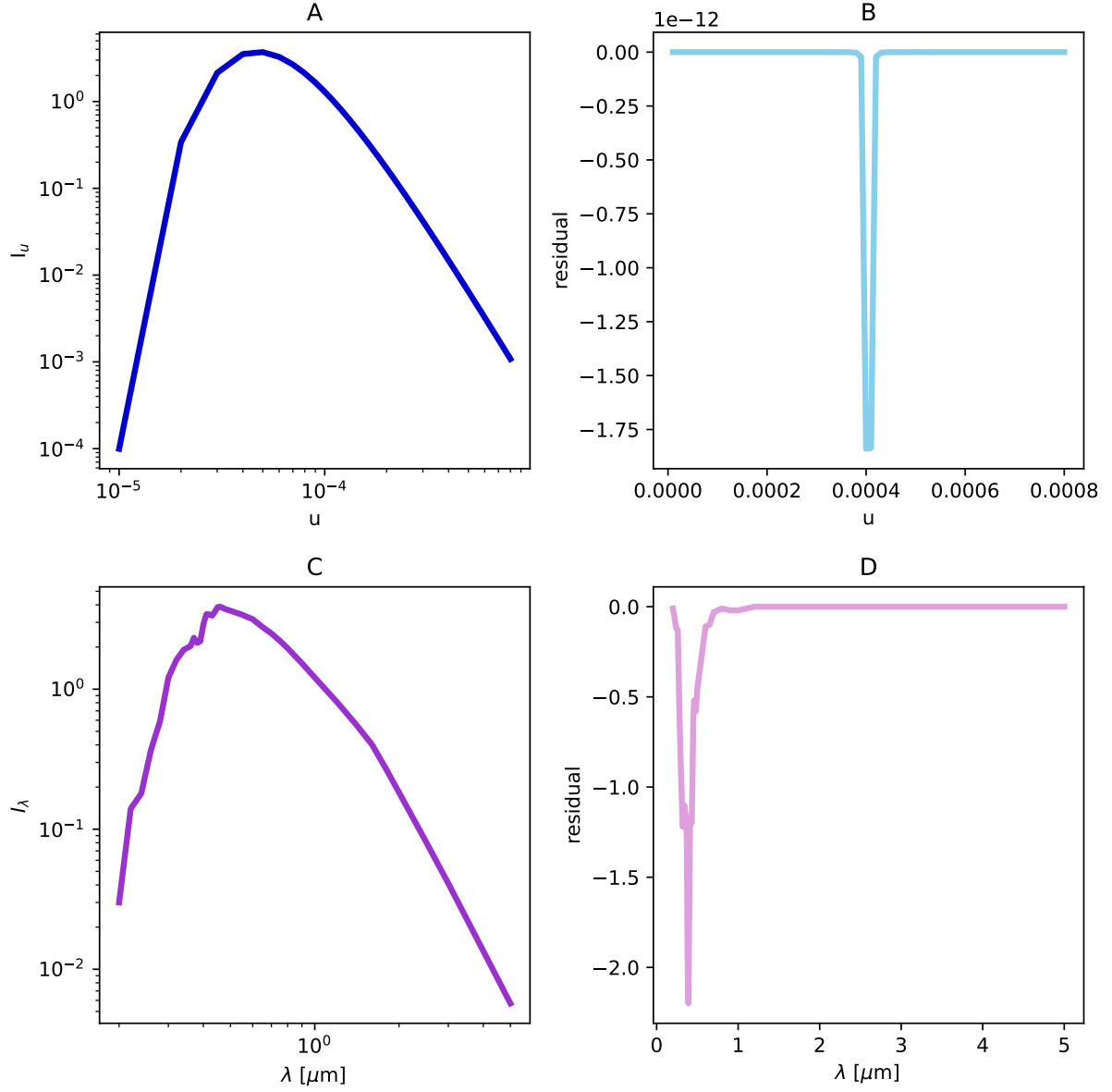


Figure 19. Panel A: Model Solar spectrum including the Na D1 absorption line. Panel B: Residual of model spectrum and model continuum spectrum (effectively the blackbody fit from part 2.4). Panel C: Observed Solar spectrum. Panel D: Residual of observed spectrum and observe continuum spectrum.